Springer

Journal of Mechanical Science and Technology 23 (2009) 2861~2870

Journal of Mechanical Science and Technology

www.springerlink.com/content/1738-494x
DOI 10.1007/s12206-009-0803-8

A new algorithm for the simulation of the boltzmann equation using the direct simulation monte-carlo method †

A. A. Ganjaei and S. S. Nourazar*

Mechanical Engineering Department, Amirkabir University of Technology, Tehran, IRAN

(Manuscript Received December 22, 2008; Revised June 9, 2009; Accepted July 5, 2009)

Abstract

A new algorithm, the modified direct simulation Monte-Carlo (MDSMC) method, for the simulation of Couette-Taylor gas flow problem is developed. The Taylor series expansion is used to obtain the modified equation of the first-order time discretization of the collision equation and the new algorithm, MDSMC, is implemented to simulate the collision equation in the Boltzmann equation. In the new algorithm (MDSMC) there exists a new extra term which takes in to account the effect of the second order collision. This new extra term has the effect of enhancing the appearance of the first Taylor instabilities of vortices streamlines. In the new algorithm (MDSMC) there also exists a second order term in time step in the probabilistic coefficients which has the effect of simulation with higher accuracy than the previous DSMC algorithm. The appearance of the first Taylor instabilities of vortices streamlines using the MDSMC algorithm at different ratios of ω/ν (experimental data of Taylor [1]) occurred at less time-step than using the DSMC algorithm. The results of the torque developed on the stationary cylinder using the MDSMC algorithm show better agreement in comparison with the experimental data of Kuhlthau [2] than the results of the torque developed on the stationary cylinder using the DSMC algorithm.

Keywords: Boltzmann equation; DSMC; Rotating cylinder; High order DSMC; Modified DSMC

1. Introduction

In the gas flow problems where the length scale of the system is comparable to the mean free path for molecules in the gas flow the concept of the continuum is no more valid, Knudsen number greater than 0.1 [3]. In this case the simulation is done using the Direct Simulation Monte-Carlo (DSMC) or the Collisional Boltzmann Equation (CBE) methods. In most cases the direct solution of the CBE is impracticable due to the huge number of molecules, however most of the time; the implementation of the DSMC is more practicable.

So far the rarefied gas flow problems are simulated using the DSMC algorithm by Vogenitz et al. [4], Stefanov et al. [5], Bird G. A. [3] & [6], Shinagawa et al. [7] and Myong [8]. The DSMC algorithm is used in the flow simulation of the previous researchers and the results of the simulations show some discrepancies when compared with the experimental data. For example Vogenitz et al. [4], studied the theoretical and experimental aspects of the rarefied supersonic flow about several simple shapes (sphere, cylinder, cone and wedge). Their results of simulation show less discrepancy at high Knudsen number than low Knudsen number when compared with measurements.

The Couette-Taylor gas flow is simulated using the DSMC algorithm by Stefanov and Cercignani [5]. The formation of the Taylor instabilities of vortices is clearly exhibited. The unsteady axially symmetric and three-dimensional Couette-Taylor flow is simulated by Bird [6]. In this work, the current status of the

† This paper was recommended for publication in revised form by Associate Editor Gihun Son

*Corresponding author. Tel.: +98 912 218 0180, Fax.: +98 21 6640 5844
E-mail address: icp@aut.ac.ir

DSMC algorithm is reviewed with particular emphasis on its range of validity, the extent of its validation against experiment, and the DSMC applications to the study of flow instabilities are discussed.

The simulation of the rarefied gas flow through circular tube of finite length in the transitional regime at both low Knudsen number and high Knudsen number are done using the DSMC algorithm by Shinagawa et al. [7] and Myong [8].

In this study we would like to develop a new algorithm to simulate the collision equation in the Boltzmann equation with higher accuracy than the previous algorithms available in the literature.

1.1 Purpose of the present work

So far the rarefied gas dynamic problems, when the Knudsen number is large enough, are simulated using the first-order time discretizations of the Boltzmann equation [3]. The Boltzmann equation is split in time in to purely convective equation (collision term is zero) and purely collision equation (convective term is zero). The collision equation is discretized in time by the first-order Euler scheme and the probabilistic interpretation of the discretized equation breaks down when the ratio $\mu\Delta t/\varepsilon$ is large enough, [9-14]. However in the present work our goal is to develop a new algorithm which considers the effects of the truncation errors in the time discretization of the first-order Euler scheme for the collision equation in order to achieve more accurate probabilistic interpretations. To achieve this goal, we write the modified equation of the first-order Euler scheme using the Taylor expansion series and then we capture the higher order truncated terms. In the present work due to the limitation of the computing time we are limited to choose only the first two terms in the Taylor expansion series. The detail of the derivation of our new algorithm which we call that modified direct simulation Monte-Carlo (MDSMC) algorithm is presented in the section 2b the MDSMC algorithm.

2. Mathematical formulations

2.1 The boltzmann equation

The Boltzmann equation is written as, [15]:

$$\frac{\partial f}{\partial t}+\mathrm{v}\cdot\nabla_{\mathrm{r}} f = \frac{1}{\varepsilon}\int_{R^3}\int_{S^2}\sigma\left(|\mathrm{v}-\mathrm{v}_*|,\Omega\right)\left(f(\mathrm{v}')f(\mathrm{v}'_*)-f(\mathrm{v})f(\mathrm{v}_*)\right)d\Omega d\,\mathrm{v}_* = \frac{1}{\varepsilon}Q(f,f) \tag{1}$$

In Eq. (1), $f(\mathrm{v})$ is the nonnegative density probability distribution function of molecule of class having the velocity of v, $f(\mathrm{v}_*)$ is the nonnegative density probability distribution function of the molecule of class having the velocity of v_*, $f(\mathrm{v}')$ is the post-collision nonnegative density probability distribution function of the molecule of class having the velocity of v', and $f(\mathrm{v}'_*)$ is the post-collision nonnegative density probability distribution function of the molecule of class having the velocity of v'_* and Ω is the angle in the spherical coordinates. The $Q(f,f)$ is the integral collision which describes the binary collisions of the molecules. The kernel σ is a non negative function which is described, [11-14]:

$$\sigma\left(|\mathrm{v}-\mathrm{v}_*|,\Omega\right)=b_\alpha(\theta)|\mathrm{v}-\mathrm{v}_*|^{\alpha}\cdot \tag{2}$$

Where, θ is the scattering angle between $\mathrm{v}-\mathrm{v}_*$ and $|\mathrm{v}-\mathrm{v}_*|\Omega$. The variable hard sphere (VHS), [3], model is often used in numerical simulation of rarefied gases, where, $b_\alpha(\theta)=C$ with C a positive constant and $\alpha=1$. The value of C is equal to (Bird, 1994), $C=\sigma_T$,where σ_T is the collision cross section and is equal $\pi d^2/4\cdot$

2.2 The MDSMC algorithm

Splitting equation 1, the Boltzmann equation, [16], into equation for the effect of collision, $\mathrm{v}\cdot\nabla_{\mathrm{r}} f\equiv 0$, and equation for the effect of convection, $Q(f,f)\equiv 0$. The equation for the effect of convection is written as, [11-14]:

$$\frac{\partial f}{\partial t}+\mathrm{v}\nabla_{\mathrm{r}} f=0\ . \tag{3}$$

And the equation for the effect of collision is written as, [11-14]:

$$\frac{\partial f}{\partial t}=\frac{1}{\varepsilon}Q(f,f)\ , \tag{4}$$

and the collision term is written as:

$$\begin{aligned}&\frac{1}{\varepsilon}Q(f,f)=\\&\int_{-\infty}^{+\infty}\int_{0}^{4\pi}\sigma_T\left|\mathrm{v}-\mathrm{v}_*\right|\left(f(\mathrm{v}')f(\mathrm{v}_*')-f(\mathrm{v})f(\mathrm{v}_*)\right)d\Omega d\,\mathrm{v}_*\\&=\int_{-\infty}^{+\infty}\int_{0}^{4\pi}\sigma_T\left|\mathrm{v}-\mathrm{v}_*\right|f(\mathrm{v}')f(\mathrm{v}_*')\,d\Omega d\,\mathrm{v}_*\\&-\int_{-\infty}^{+\infty}\int_{0}^{4\pi}\sigma_T\left|\mathrm{v}-\mathrm{v}_*\right|f(\mathrm{v})f(\mathrm{v}_*)\,d\Omega d\,\mathrm{v}_*\\&=\frac{1}{\varepsilon}\left[P(f,f)-\mu(\mathrm{v})f\right]\end{aligned}\tag{5}$$

Where, $\mu(\mathrm{v})=\int_{-\infty}^{+\infty}\int_{0}^{4\pi}\sigma_T\left|\mathrm{v}-\mathrm{v}_*\right|f(\mathrm{v}_*)d\Omega d\,\mathrm{v}_*=\int_{-\infty}^{+\infty}\sigma_T\left|\mathrm{v}-\mathrm{v}_*\right|d\Omega$ $\int_{0}^{4\pi}f(\mathrm{v}_*)d\,\mathrm{v}_*=\kappa\rho/m$ is the mean collision frequency for the molecules having velocity v , ρ is the density of the gas, m is the mass of a molecule of the gas, κ is a molecular constant $\kappa=\int_0^{4\pi}\sigma_T\left|\mathrm{v}-\mathrm{v}_*\right|d\Omega$ and $\rho/m=\int_{-\infty}^{+\infty}f(\mathrm{v}_*)d\,\mathrm{v}_*$ [17]. In special case in which $\sigma_T\left|\mathrm{v}-\mathrm{v}_*\right|$ is independent of $\left|\mathrm{v}-\mathrm{v}_*\right|$ (Maxwellian molecules), we have:

$$\mu(\mathrm{v})=\mu=\frac{\kappa\rho}{m}.\tag{6}$$

Substituting Eq. (6) into Eq. (5) and then into Eq. (4):

$$\frac{\partial f}{\partial t}=\frac{1}{\varepsilon}Q(f,f)=\frac{1}{\varepsilon}\left[P(f,f)-\mu f\right].\tag{7}$$

The first order time discretization of Eq. (7) is written as:

$$f^{n+1}=\left(1-\frac{\mu\Delta t}{\varepsilon}\right)f^n+\frac{\mu\Delta t}{\varepsilon}\frac{P\left(f^n,f^n\right)}{\mu}.\tag{8}$$

The probabilistic interpretation of Eq. (8) is the following. In order a particle is sampled from f^{n+1}, a particle is sampled from f^n with probability of $\left(1-\mu\Delta t/\varepsilon\right)$ and a particle is sampled from $P\left(f^n,f^n\right)/\mu$ with probability of $\mu\Delta t/\varepsilon$. It is to be noted that the above probabilistic interpretation fails if the ratio of $\mu\Delta t/\varepsilon$ is too large because the coefficient of f^n on the right hand side may become negative, [9-14].

In our algorithm, we write for f^{n+1} Taylor series expansion as:

$$f^{n+1}=f^n+\Delta t\left.\frac{\partial f}{\partial t}\right|^n+\frac{(\Delta t)^2}{2!}\left.\frac{\partial^2 f}{\partial t^2}\right|^n+O(\Delta t)^3.\tag{9}$$

The second order derivative, $\partial^2 f/\partial t^2$, in equation 9 is written as:

$$\begin{aligned}&\left.\frac{\partial^2 f}{\partial t^2}\right|^n=\frac{\partial}{\partial t}\left(\frac{\partial f}{\partial t}\right)\Bigg|^n=\\&\frac{\partial}{\partial t}\left(\frac{1}{\varepsilon}\left[P\left(f^n,f^n\right)-\mu f^n\right]\right)\Bigg|^n=\\&\left.\frac{1}{\varepsilon}\frac{\partial P\left(f^n,f^n\right)}{\partial t}-\frac{\mu}{\varepsilon}\frac{\partial f}{\partial t}\right|^n=\\&\frac{1}{\varepsilon}\frac{\partial P\left(f^n,f^n\right)}{\partial t}-\frac{\mu}{\varepsilon}\left(\frac{1}{\varepsilon}\left[P\left(f^n,f^n\right)-\mu f^n\right]\right)\\&=\frac{1}{\varepsilon}\frac{\partial P\left(f^n,f^n\right)}{\partial t}-\frac{\mu}{\varepsilon^2}P\left(f^n,f^n\right)+\frac{\mu^2}{\varepsilon^2}f^n.\end{aligned}\tag{10}$$

Substituting equation10 for the value of $\partial^2 f/\partial t^2$ and equation 7 for the value of $\partial f/\partial t$ into Eq. (9):

$$\begin{aligned}&f^{n+1}=f^n+\frac{\Delta t}{\varepsilon}\left[P\left(f^n,f^n\right)-\mu f^n\right]+\\&\frac{(\Delta t)^2}{2!}\left(\frac{1}{\varepsilon}\frac{\partial P\left(f^n,f^n\right)}{\partial t}-\frac{\mu}{\varepsilon^2}P\left(f^n,f^n\right)\right.\\&\left.+\frac{\mu^2}{\varepsilon^2}f^n\right)+O(\Delta t)^3.\end{aligned}\tag{11}$$

The $P\left(f^n,f^n\right)=\int_{-\infty}^{+\infty}\int_{0}^{4\pi}\sigma_T\left|v-v_*\right|f^n(v')f(v_*')d\Omega\,dv_*$ is the bilinear operator describing the collision effect of two molecules. The time derivative of $P\left(f^n,f^n\right)$ is written as:

$$\begin{aligned}&\Rightarrow\frac{\partial P\left(f^n,f^n\right)}{\partial t}=\\&\int_{-\infty}^{+\infty}\int_{0}^{4\pi}\sigma_T\left|v-v_*\right|\frac{\partial f^n(v')}{\partial t}f(v_*')d\Omega\,dv_*.\end{aligned}\tag{12}$$

The time discretization of $\partial P\left(f^n,f^n\right)/\partial t$ is written as:

$$\frac{\partial P\left(f^n,f^n\right)}{\partial t}= \int_{-\infty}^{+\infty}\int_{0}^{4\pi}\sigma_T\left|\mathrm{v}-\mathbf{v}_*\right|\left(\frac{f_1^n\left(\mathrm{v}'\right)-f^n\left(\mathrm{v}'\right)}{\Delta t}\right)f\left(\mathrm{v}_*'\right)d\Omega d\,\mathrm{v}_* = \frac{1}{\Delta t}\left\{\int_{-\infty}^{+\infty}\int_{0}^{4\pi}\sigma_T\left|\mathrm{v}-\mathbf{v}_*\right|f_1^n\left(\mathrm{v}'\right)f\left(\mathrm{v}_*'\right)d\Omega d\,\mathrm{v}_* - \int_{-\infty}^{+\infty}\int_{0}^{4\pi}\sigma_T\left|\mathrm{v}-\mathbf{v}_*\right|f^n\left(\mathrm{v}'\right)f\left(\mathrm{v}_*'\right)d\Omega d\,\mathrm{v}_*\right\} \tag{13}$$

Substituting for $P\left(f^n,f^n\right)=\int_{-\infty}^{+\infty}\int_{0}^{4\pi}\sigma_T\left|v-v_*\right|f^n\left(v'\right)f\left(v_*'\right)d\Omega\,dv_*$ into Eq. (13):

$$\frac{\partial P\left(f^n,f^n\right)}{\partial t}=\frac{1}{\Delta t}\left\{P\left(f_1^n,f^n\right)-P\left(f^n,f^n\right)\right\}. \tag{14}$$

Substituting Eq. (14) into Eq. (11):

$$f^{n+1}=f^n+\frac{\mu\Delta t}{\varepsilon}\left[\frac{P\left(f_1^n,f^n\right)}{\mu}-f^n\right]+\frac{\left(\Delta t\right)^2}{2!}\left(\frac{\mu}{\varepsilon\Delta t}\left\{\frac{P\left(f_1^n,f^n\right)}{\mu}-\frac{P\left(f_1^n,f^n\right)}{\mu}\right\}-\frac{\mu^2}{\varepsilon^2}\frac{P\left(f^n,f^n\right)}{\mu}+\frac{\mu^2}{\varepsilon^2}f^n\right)+O\left(\Delta t\right)^3, \tag{15}$$

where $f_1^n=P\left(f^n,f^n\right)/\mu$ .Rearranging and truncating terms higher than the second order in Eq. (15):

$$f^{n+1}=\left(1-\frac{\mu\Delta t}{\varepsilon}+\frac{\mu^2\left(\Delta t\right)^2}{2\varepsilon^2}\right)f^n+\left(\frac{\mu\Delta t}{2\varepsilon}-\frac{\mu^2\left(\Delta t\right)^2}{2\varepsilon^2}\right)\frac{P\left(f^n,f^n\right)}{\mu}+\frac{\mu\Delta t}{2\varepsilon}\frac{P\left(f_1^n,f^n\right)}{\mu}. \tag{16}$$

The probabilistic interpretation of Eq. (16) is the following. In order a particle is sampled from f^{n+1}, a particle is sampled from f^n with probability of $\left(1-\mu\Delta t/\varepsilon+\mu^2\left(\Delta t\right)^2/2\varepsilon^2\right)$, a particle is sampled from $P\left(f^n,f^n\right)/\mu$ with probability of $\left(\mu\Delta t/2\varepsilon-\mu^2\left(\Delta t\right)^2/2\varepsilon^2\right)$ and a particle is sampled from $P\left(f_1^n,f^n\right)/\mu$ with probability of $\mu\Delta t/2\varepsilon$. Comparing equation 16, the new algorithm (MDSMC), with equation 8 (the DSMC algorithm) reveals two facts as follows: 1) Eq. (17), the new algorithm (MDSMC), consists of three terms that are sampled probabilistically, however Eq. (8) (the DSMC algorithm) consists of two terms that are sampled probabilistically, the third extra term in Eq. (16), $P\left(f_1^n,f^n\right)/\mu$, is interpreted as the collision between the particles sampled from f^n and the particles sampled from $P\left(f^n,f^n\right)/\mu$ 2) the probabilistic coefficients in Eq. (17), the new algorithm (MDSMC), consist of the second order terms in time step however the probabilistic coefficients in Eq. (8) (the DSMC algorithm) consist of the first order terms in time step.

3. Analytical solutions

The energy E of a particle in an axially symmetric gas flow inside a rotating cylinder is given as, [18],

$$E\left(r\right)=\frac{1}{2}I\omega^2=\frac{1}{2}mr^2\omega^2. \tag{17}$$

The rotational effect is the same of additional external field acting on the system and may be written as:

$$U\left(r\right)=-\frac{1}{2}I\omega^2=-\frac{1}{2}mr^2\omega^2. \tag{18}$$

Using the Boltzmann distribution for the particle number density and substituting for $U\left(r\right)$ from Eq. (18):

$$n\left(r\right)=A\exp\left(-\frac{U\left(r\right)}{kT}\right)=A\exp\left(\frac{mr^2\omega^2}{2kT}\right), \tag{19}$$

the normalization factor A in Eq. 19, is determined by $N=\int n\left(r\right)dV$:

$$N=\int_0^R\int_0^{2\pi}A\exp\left(\frac{mr^2\omega^2}{2kT}\right)rdrd\varphi=\frac{2\pi AkT}{m\omega^2}\left(\exp\left(\frac{mR_2^2\omega^2}{2kT}\right)-1\right). \tag{20}$$

Then the normalization factor A is $\frac{Nm\omega^2}{2\pi kT}\left(\exp\left(\frac{mR^2\omega^2}{2kT}\right)-1\right)^{-1}$.

Substituting for A into Eq. (20):

$$n(r)=\frac{Nm\omega^2}{2\pi kTL}\frac{\exp\left(\frac{m\omega^2 r^2}{2kT}\right)}{\exp\left(\frac{m\omega^2 R^2}{2kT}\right)-1}. \quad (21)$$

Where, N is the total number of molecules, m is the mass of a molecule of gas, ω is the angular velocity, k is the Boltzmann constant, T is the absolute temperature, L is the length of the cylinder, R is the cylinder radius and r is the radial distance.

4. The numerical procedures

4.1 The DSMC Algorithm (the VHS collision model molecules):

• for all particles
- Compute an upper bound $\bar{\sigma}=\max\left[\left(\pi d^2\left|\mathrm{v}_i-\mathrm{v}_j\right|\right)/4\right]$ for the cross section, $\bar{\sigma}$ is updated in each collision.
- Set $\mu=4\pi\bar{\sigma}$.
- Set $N_c=Iround\left(\mu N\Delta t/(2\varepsilon)\right)$.
- Select $2N_c$ dummy collision pairs (i,j) uniformly among all possible pairs, and for those.
- Compute the relative cross section $\sigma_{ij}=\pi d^2\left|\mathrm{v}_i-\mathrm{v}_j\right|/4$.
- Generate uniform random numbers *Rand*.
- If $Rand<\sigma_{ij}/\bar{\sigma}$
  · Perform the collision between i and j, and compute the post-collision velocities v_i^* and v_j^*.
  · Set $\mathrm{v}_i^{n+1}=\mathrm{v}_i^*$, $\mathrm{v}_j^{n+1}=\mathrm{v}_j^*$.
  · else
  · Set $\mathrm{v}_i^{n+1}=\mathrm{v}_i^n$, $\mathrm{v}_j^{n+1}=\mathrm{v}_j^n$.
  · Set $\mathrm{v}_i^{n+1}=\mathrm{v}_i^n$ for the N_i-2N_c particles that have not been selected.
  · End for

During each step, all the other N_i-2N_c particle velocities remain unchanged.

4.2 The MDSMC Algorithm (the VHS collision model molecules):

• for $n_t=1$ *to* $\mathrm{n}_{\mathrm{tot}}$
- Compute an upper bound, $\bar{\sigma}$.
- Set $\mu=4\pi\bar{\sigma}$.
- Compute

$$N_{c_1}=Iround\left(\frac{N}{2}\left(\frac{\mu\Delta t}{2\varepsilon}+\frac{\mu^2(\Delta t)^2}{2\varepsilon^2}\right)+\frac{N}{4}\left(\frac{\mu\Delta t}{2\varepsilon}\right)\right).$$

- Select $2N_{c_1}$ dummy collision pairs (i,j) uniformly among all possible pairs.
- Compute the relative cross section σ_{ij}.
- Generate uniform random numbers (*Rand*).
- If $Rand<\sigma_{ij}/\bar{\sigma}$
  · Perform the collision between i and j, and compute the post-collision velocities v_i^* and v_j^*.
- Set $N_{c_2}=Iround\left(\frac{N}{2}\left(\frac{\mu\Delta t}{2\varepsilon}\right)\right)$.
- Select N_{c_2} particles among those that have not collided and select N_{c_2} particles among those that have collided.
- Compute the relative cross section σ_{ij}.
- Generate uniform random numbers (*Rand*).
- If $Rand<\sigma_{ij}/\bar{\sigma}$
  · Perform the collision between i and j, and compute the post-collision velocities v_i^* and v_j^*.
  · Set $\mathrm{v}_i^{n+1}=\mathrm{v}_i^n$ for all the $N-2N_{c_1}-N_{c_2}$ particles that have not been selected.
• End for

5. Discussions of results

5.1 Description of case study problems

In order to validate our new algorithm we consider three different case study problems, in the first case study problem the number density of argon in a rotating cylinder is simulated using the MDSMC and DSMC algorithms, with 7.870515094×10^{20} real molecules, 120000 model molecules and 50000 (1000×50) total number of cells, and the results of the simulation are compared with the analytical solution. The radius of the cylinder is $0.01m$ and its length is $0.2m$ and rotates with angular velocity of $15900\,rev/s$. The gas inside the cylinder is Argon (Ar) with the initial temperature of $300K$ and the initial pressure of $3.0Pa$ absolute**.** In the second and third case study problems the Couette-Taylor flow is simulated using the MDSMC and DSMC algorithms, with 2.414370721×10^{21} real molecules, 120000 model molecules and 5000 (250×20) total number of cells, and the results of the simulation are compared with the experimental data of Taylor, G. I., [1] and Kuhlthau, A. R., [2]. For the comparison purposes we choose the same case study problems depicted by Taylor, G. I., [1] and Kuhlthau, A., [2] respectively.

5.2 Comparisons of the number density results with the analytical solution

Fig. 1 shows the comparison of the analytical solution of the number density of the argon gas inside a rotating cylinder with the results of the MDSMC and the DSMC simulations. The comparison of the results of the number density using the MDSMC algorithm with the analytical solution shows closer agreement than the results of the number density using the DSMC algorithm. The agreement between our results of the number density using the MDSMC algorithm is more pronounced than the results of the number density using the DSMC algorithm in the region closer to the center of the cylinder. Furthermore, the fluctuations of the number density results using the MDSMC algorithm are less than the fluctuations of the number density results using the DSMC algorithm in the region closer to the center of the cylinder.

Figs. 2(a), 2(b), 2(c) and 2(d) show the results of the streamlines and the density contours using the MDSMC and the DSMC algorithms and the results of the streamlines and the temperatures contours using the MDSMC and the DSMC algorithms respectively. The results of the streamlines, the density contours and the temperatures using the MDSMC have less fluctuation than the results of the DSMC simulations. This is in agreement with the results of the simulation using the MDSMC and the DSMC algorithms for the number density in Fig. 1.

5.3 Comparisons of the results of Couette-Taylor flow simulations with experiments of Taylor

The first Taylor instabilities of vortices streamlines

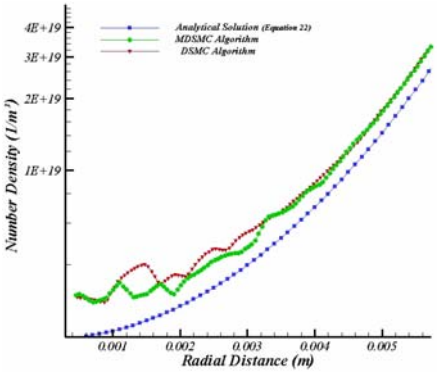

Fig. 1. Comparison of the analytical solution of the number density with the results of the MDSMC and the DSMC algorithms.

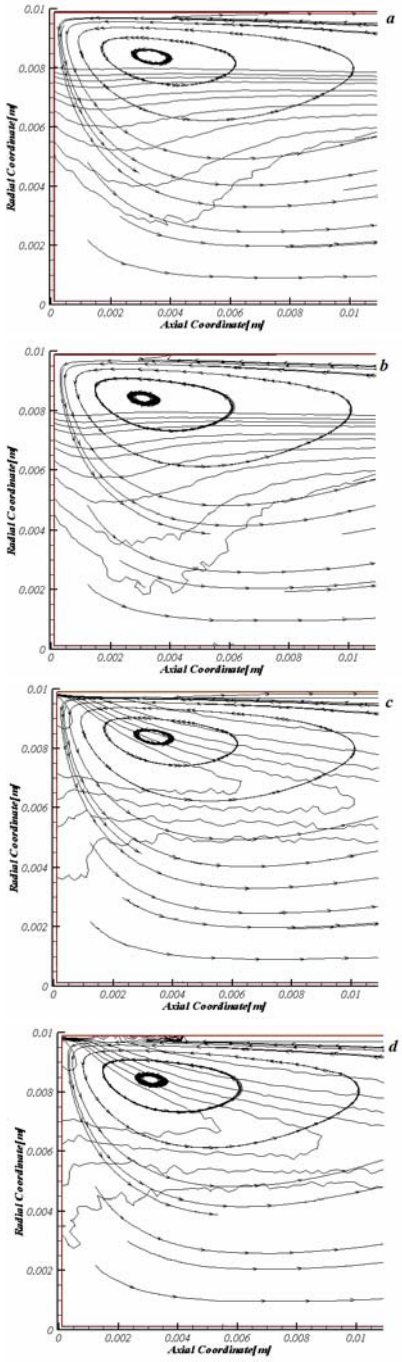

Fig. 2. the streamlines, the constant density contours and the constant temperature contours: (a) the streamlines and the constant density contours using the MDSMC algorithm, (b) the streamlines and the constant density contours using the DSMC algorithm, (c) the streamlines and the constant temperature contours using the MDSMC algorithm, (d) the streamlines and the constant temperature contours using the DSMC algorithm.

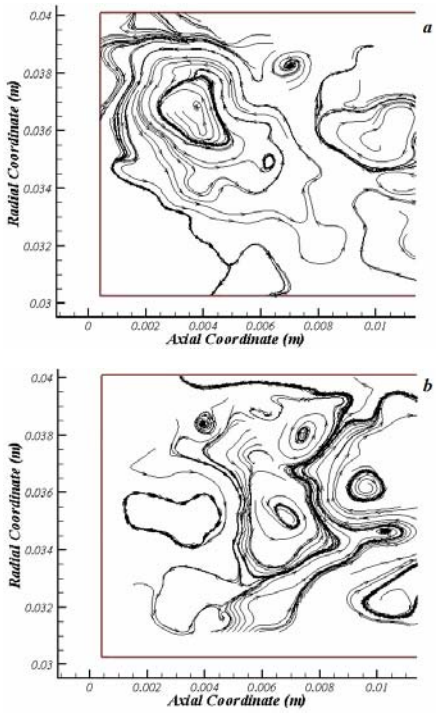

Fig. 3. Streamlines: (a) using the MDSMC algorithm at Ta=2.797295199×10-5 after 16000 iterations, (b) using the DSMC algorithm at Ta=2.797295199×10-5 after 24000 iterations.

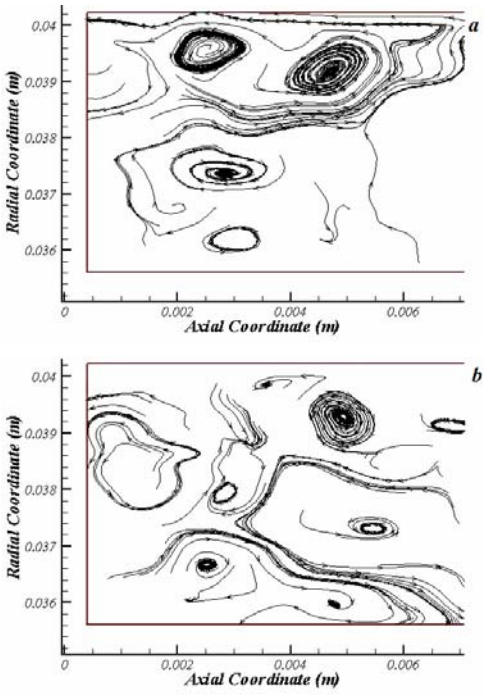

Fig. 4. Streamlines: (a) using the MDSMC algorithm at Ta=1.984493354×10-5 after 10000 iterations, (b) using the DSMC algorithm at Ta=1.984493354×10-5 after 24000 iterations.

in the Taylor, [1] experiment appear at the ratios of $\omega/\nu = 30.3 rad/m^2$, $\omega/\nu = 70.7 rad/m^2$ and $\omega/\nu = 189.2$ rad/m^2 , where these values of the ratio ω/ν correspond to three geometries in the Taylor, [1] experiment as follows; the first geometry consists of $R_1 = 3.0cm$, $R_2 = 4.035cm$ and L=20.32cm, the second geometry consists of $R_1 = 3.55cm$, $R_2 =$ $4.035cm$ and L=20.32cm and the third geometry consists of $R_1 = 3.8cm$, $R_2 = 4.035cm$ and L=20.32cm, where R_1 is the outer radius of the inner cylinder, R_2 is the inner radius of the outer cylinder and L is the height of the cylinder. Figs. 3(a) and 3(b) show the results of the Taylor instabilities of vortices streamlines at the ratio of $\omega/\nu = 30.0 rad/m^2$ using the MDSMC and the DSMC algorithms respectively. The first Taylor instabilities of vortices streamlines using the MDSMC and the DSMC algorithms appear at the ratio of $\omega/\nu = 30.0 rad/m^2$, whereas in the experiment of Taylor, [1] the first Taylor instabilities of vortices streamlines appear at the ratio of $\omega/\nu = 30.3 rad/m^2$. The results of the Taylor instabilities of vortices streamlines using the MDSMC algorithm appear after 16000 iterations, whereas the

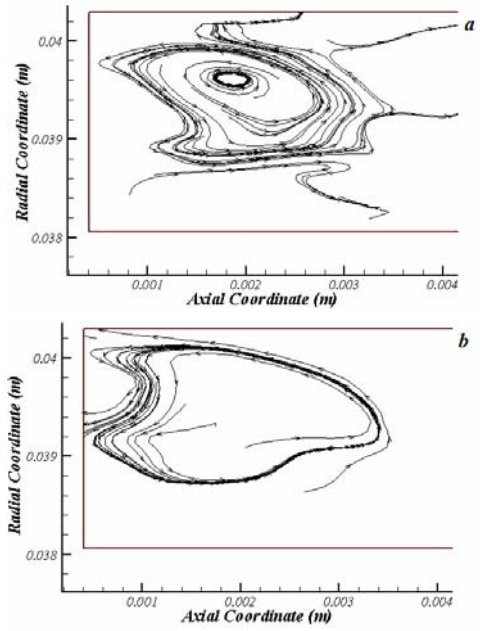

Fig. 5. Streamlines: (a) using the MDSMC algorithm at Ta=1.743022053×10-5 after 10000 iterations, (b) using the DSMC algorithm at Ta=1.743022053×10-5 after 23000 iterations.

results of Taylor instabilities of vortices streamlines using the DSMC appear after 24000 iterations. Figs. 4(a) and 4(b) show the results of the Taylor instabilities of vortices streamlines at the ratio of $\omega/\nu = 70.7\,rad/m^2$ using the MDSMC and the DSMC algorithms respectively. The first Taylor instabilities of vortices streamlines using the MDSMC and the DSMC algorithms appear at the ratio of $\omega/\nu = 70.0\,rad/m^2$, whereas in the experiment of Taylor, [1] the first Taylor instabilities of vortices streamlines appear at the ratio of $\omega/\nu = 70.0\,rad/m^2$. The first Taylor instabilities of vortices streamlines using the MDSMC algorithm appear after 10000 iterations, whereas the first Taylor instabilities of vortices streamlines using the DSMC appear after 24000 iterations. Figs. 5(a) and 5(b) show the results of the Taylor instabilities of vortices streamlines at the ratio of $\omega/\nu = 189.0\,rad/m^2$ using the MDSMC and the DSMC algorithms respectively. The first Taylor instabilities of vortices streamlines using the MDSMC and the DSMC algorithms appear at the ratio of $\omega/\nu = 189.0\,rad/m^2$, whereas in the experiment of Taylor the first Taylor instabilities of vortices streamlines appear at the ratio of $\omega/\nu = 189.2\,rad/m^2$. The first Taylor instabilities of vortices streamlines using the MDSMC algorithm appear after 10000 iterations, whereas the first Taylor instabilities of vortices streamlines using the DSMC appear after 23000 iterations. Therefore, the effect of the new algorithm (MDSMC) in the simulation is to enhancing the appearance of the Taylor instabilities of vortices streamlines.

5.4 Comparisons of the results of Couette-Taylor flow simulations with experiments of Kuhlthau

The torque developed on the outer cylinder in the Couette-Taylor flow is measured by Kuhlthau, [2]. The geometry of Couette-Taylor flow in Kuhlthau, [2] experiment consists of $R_1 = 5.08cm$, $R_2 = 6.35cm$ and L=3.81cm where R_1 is the outer radius of the inner cylinder, R_2 is the inner radius of the outer cylinder and L is the height of the cylinder. The pressure of the gas in the space between the two cylinders is 100 μm Hg and the inner cylinder rotates at six different angular velocities of 400, 800, 1000, 1200, 1400 and 1600 Rev/*Sec*. The results of the torque developed on the outer cylinder using the MDSMC and the DSMC algorithms are compared with the experimental data of Kuhlthau, [2]. Fig. 6 shows the comparison of the experimental data of the developed torque on the stationary cylinder with the results of simulation using the MDSMC and DSMC algorithms at six different angular velocities of 400, 800 1000, 1200, 1400 and 1600 Rev/*Sec*. The comparison of the present results of simulation with the experimental data of Kuhlthau, [2] show that the results of simulation using the MDSMC are in closer agreement than the results of simulation using the DSMC algorithm. Table 1 shows the error associated with the torque developed on the stationary cylinder using the MDSMC and DSMC algorithms at six different angular velocities of 400, 800, 1000, 1200, 1400 and 1600 Rev/*Sec* when compared with the experimental data .The errors associated with the results of the torque using the MDSMC are less than the errors of the results of the torque using the DSMC when com-

Table 1. shows the comparison of the results of the torque developed on the stationary cylinder using the MDSMC and DSMC algorithms with the experimental data of Kuhlthau (1960).

Rotational Velocity *(R/S)*	Calculated Torque of the MDSMC $(N.m)\times10^4$	Calculated Torque of the DSMC $(N.m)\times10^4$	Measured Torque by Kuhlthau (1960) $(N.m)\times10^4$	Error in Calculation MDSMC with Measurement	Error in Calculation DSMC with Measurement
400	*1.62*	*1.77*	*1.6949*	*4.419%*	*4.4309%*
800	*3.37422*	*3.76574*	*3.5593*	*5.2%*	*5.8%*
1000	*3.991*	*4.6409*	*4.3051*	*7.3%*	*7.8%*
1200	*4.92*	*6.09*	*5.3898*	*8.71%*	*12.99%*
1400	*5.99*	*7.26*	*6.4407*	*7.0%*	*12.72%*
1600	*8.093*	*9.4611*	*8.7119*	*7.1%*	*8.6%*

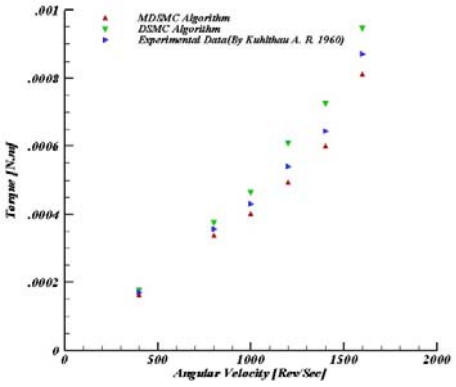

Fig. 6. Comparison of experimental data of the developed torque on the stationary cylinder using the MDSMC and DSMC algorithms.

pared with the experimental data.

6. Conclusions

Comparing the results of the simulation with the experimental data shows that the new algorithm developed in the present work (the MDSMC algorithm) has the capability of simulating the Couette-Taylor gas flow problem with higher accuracy than the previous DSMC algorithm. The appearance of the first Taylor instabilities of the vortices streamlines using the MDSMC algorithm is enhanced when compared with the appearance of the first Taylor instabilities of the vortices streamlines using the DSMC algorithm. These are due to the facts that, in the new algorithm (MDSMC) there exists a new extra term $P\left(f_1^n, f^n\right)/\mu$ which takes in to account the effect of the collision between the particles sampled from f^n and the particles sampled from $P\left(f^n, f^n\right)/\mu$ which we call that the second order collision term. This new extra term has the effect of enhancing the appearance of the first Taylor instabilities of vortices streamlines. Finally in the new algorithm (MDSMC) there exists a second order term in time step in the probabilistic coefficients which has the effect of simulation with higher accuracy than the previous DSMC algorithm.

References

[1] G. I. Taylor, Stability of a Viscous Liquid Contained between Two Rotating Cylinders, *Phil. Trans., Ser. A*, 223 (1923) 289-347.

[2] A. R. Kuhlthau, Recent Low Density Experiments using Rotating Cylinder Techniques, *In Proceeding of the first international symposium on rarefied gas dynamics, (ed. F.M. Deuienne)*, (1960), 192-200, Pergamon, London.

[3] G. A. Bird, *Molecular Gas Dynamics and the Direct Simulation of Gas Flows*, Oxford Univ. Press, London (1994).

[4] F. W. Vogenitz, G. A. Bird, J. E. Broadwel and H. Rungaldier, Theoretical and Experimental Study of Rarefied Supersonic Flows about Several Simple Shapes, *AIAA Journal*, 6 (12) (1968) 2388-2394.

[5] S. Stefanov and C. Cercignani, Monte Carlo Simulation of the Taylor-Couette Flow of a Rarefied Gas, *Journal of Fluid Mechanics*, 256 (1993) 199-213.

[6] G. A. Bird, Recent Advances and Current Challenges for DSMC, *Computers and Mathematics with Applications*, 35 (1-2) (1998) 1-14.

[7] H. Shinagawa, H. Setyawan, T. Asai, Y. Sugiyama and K. Okuyama, An experimental and theoretical investigation of rarified gas flow through circular tube of finite length, *Pergamon, Chemical Engineering Science*, 56 (2002) 4027-4036.

[8] R. S. Myong, A generalized hydrodynamic computational model for rarified and micro scale gas flows, *Journal of Computational Physics*, 195, (2004), 655-676.

[9] K. Nanbu, Direct Simulation Scheme Derived From the Boltzmann Equation, *Journal of the Physical Society of Japan*, 49 (1980) 2042-2049.

[10] H. Babovsky, On a Simulation Scheme for the Boltzmann Equation, *Mathematical Method in the Applied Sciences*, 8 (1986) 223-233.

[11] L. Pareschi and R. E. Calfisch, An Implicit Monte-Carlo Method for Rarefied Gas Dynamics, *J. Comput. Phys.*, (1999), 154, 90.

[12] L. Pareschi and G. Russo, Time Relaxed Monte-Carlo Methods for the Boltzmann Equation, *SIAM J. Sci. Comput.,* 23, (2001), 1253-1273.

[13] L. Pareschi and S. Trazzi, Asymptotic Preserving Monte Carlo Methods for the Boltzmann Equation, *Transport Theory Statist. Phys.*, 29, (2005), pp.415-430.

[14] L. Pareschi and S. Trazzi, Numerical Solution of the Boltzmann Equation by Time Relaxed Monte-Carlo (TRMC) Method, *International Journal of Numerical Method in Fluids*, 48 (2005) 947-983.

[15] C. Cercignani, *The Boltzmann Equation and Its Applications*, Lectures Series in Mathematics, 68, Springer-Verlag, Berlin, New York, (1988).

[16] E. Gabetta, L. Pareschi and G. Toscani, Relaxation Schemes for Nonlinear Kinetic Equations, *SIAM J.*, Number. Anal., 34 (1997) 2168-2194.

[17] E. Wild, On Boltzmann's Equation in the Kinetic Theory of Gases, *Proc. Camb. Phil. Soc.*, 47 (1951) 602-609.

[18] L. Y. Kuo, *Problems and solutions on Thermodynamics and Statistical Mechanics*, World Scientific Publication, (1990).

Dr. S. S. Nourazar received his B.Sc. degree from Amirkabir University of Technology in Tehran, Iran. Then he proceeded his graduate studies in Canada and received the M. Sc. and PhD degrees in Mechanical engineering from Ottawa University in Canada. Dr. Nourazar is acting now as assistant professor in Mechanical Engineering Department of Amirkabir University of Technology. The research interests of Dr. Nourazar are the CFD in compressible and incompressible turbulent nonreactive flow as well as rarefied gas dynamics.

A. A. Ganjaei received his B.Sc. degree from Science & Technology of Iran University in Tehran, Iran. Then he proceeded his graduate studies in Amirkabir University of Technology and received the M. Sc. degrees in Mechanical engineering. A. A. Ganjaei is studying now as PhD student in Mechanical Engineering Department of Amirkabir University of Technology. The research interests of Ganjaei are the CFD in compressible and incompressible turbulent nonreactive flow as well as rarefied gas dynamics.